```
allowing for rearrangements in the second term, \textbf{(Lin2)},
```

```
\lstick{\ket{0}} & \gate{\hat{H}} & \ctrl{3} & \ctrl{1} \\\lstick{\ket{0}} & \gate{\hat{H}} & \qw & \ctrl{1} \\\
```

\multigate{3}{\mathrm{Ancilla}}

\ghost{\mathrm{Ancilla}}

\draw[thick,draw=purple] plot [smooth,tension=1.5] coordinates{(-1.66,-2.2) (-1.6,-1.9) (-1.5,-2.1) (-1.5,-1.9) (-1.3,-1.4) (-0.8,-1.2) (-1.2, -1.2) (-1.3,-1.6) (-0.88,-1.7) (-0.89,-2.3) (-0.01,-1.25) (-0.3,1.2) (-0.7,1.4) (-0.8,1.6) (-0.9,1.7) (-0.95,2.0) (0.07,0.9) (0.01,1.1) (0.03,0.8) (0.09,0.7) (0.1,0.8) (0.2,0.4) (1.5,-0.355555) (0.9,-0.02) (-0.3,-0.01) (-0.3,-0.2) (-0.5,0.3) (-2.2,2.1) (-2.1,1.9) (-2.4,1.8) (-2.5,0.6) (-2.8,-0.2) (-3.1,-0.5) (-3.4,0.3) (-3.6,-1.5) (-2.3,-1.7869) (-2.7,-1.7) (-2.8,-2.3) (-3.6,-2.6)};

\draw[thick,draw=purple] plot [smooth,tension=1.5] coordinates{(-1.66,-2.2) (-1.6,-1.9) (-1.5,-2.1) (-1.5,-1.9) (-1.3,-1.4) (-0.8,-1.2) (-1.2, -1.2) (-1.3,-1.6) (-0.88,-1.7)

(-0.89, -1.7)

 $\begin{array}{lll} (-0.01,-1.25) & (-0.3,1.2) & (-0.7,1.4) & (-1,1.6) & (-0.9,1.7) & (-0.95,2.0) & (0.07,0.9) & (0.01,1.1) & (0.03,0.8) \\ (0.09,0.7) & (0.1,0.8) & (0.2,0.4) & (-0.7,1) & (0.9,-0.02) & (-0.3,-0.01) & (-0.3,-0.2) & (-0.5,0.3) & (-2.2,2.1) \\ (-2.1,1.9) & (-2,1.8) & (-2.5,0.6) & (-2.8,-0.2) & (-3.1,-0.5) & (-3.4,0.3) & (-3.6,-1.5) & (-2.3,-1.7869) & (-2.7,-1.7) \\ (-2.8,-2.3) & (-3.6,-2.6) \end{array}$

 $\frac{x^{3i+2}_1}{2i^2(i+1)(3i+2)} + \frac{x^{3i+2}_1}{2i^2(i+1)(2i+1)}$

\begin{figure}[t]

\begin{center}

\begin{tikzpicture}[spy using outlines={circle,red,magnification=1.7,size=7.3cm, connect spies}]

```
1:$4_{j+\delta^{\prime}}}, label=side 2:$5_{j+\delta^{\prime}}}, label=side
3:$6 {j+\delta^{\prime}}$,
  label=side 4:$1 {j+\delta^{\prime}}$, label=side 5:$2 {j+\delta^{\prime}}$, label=side
6:$3 {j+\delta^{\prime}}$,draw=yellow] (reg2) at (-2.2,0){};
  \node[regular polygon, regular polygon sides=6, minimum width=6cm,label=side
1:$4 {j+2\delta^{\prime}}$, label=side 2:$5 {j+2\delta^{\prime}}$, label=side
3:$6_{j+2\delta^{\prime}}$,
  label=side 4:$1 {j+2\delta^{\prime}}$, label=side 5:$2 {j+2\delta^{\prime}}$, label=side
6:$3_{j+2\cdot (-1.2,0)}, draw=gray] (reg2) at (-1.2,0)};
  \node[regular polygon, regular polygon sides=6, minimum width=6cm,draw=blue] (reg1) at
(-3.2,0){};
\spy on (0.2,-1.1) in node [left] at (9,4.7);
\draw (-5,-2.6) -- (10,-2.6){};
\draw[thick,draw=red] plot [smooth,tension=1.5] coordinates{(-1.65,0.00000001) (-1.0,-0.4)
(-1.5, -0.00004) (-1.2, -0.1) (-0.9, -0.3) (-0.6, -0.3) (-0.8, -0.4) (-0.68, -0.00002) (-0.5, -0.00003)
(-0.5444, -0.3) (-0.4, -1.3) (-0.35, -1.45) (-0.4, -2) (-0.5, -1.3) (-2.1, -0.3) (-2.1, 0.1) (-2.2, -0.2)
(-1.3, -0.8) (-1.8, -1.6) (-1.9, -2.2) (-2.7, -2.6);
\draw (-5,-2.6) -- (10,-2.6){};
\draw[thick,draw=purple] plot [smooth,tension=1.5] coordinates{(-1.66,-2.2) (-1.6,-1.9) (-1.5,-2.1)
(-1.5,-1.9) (-1.3,-1.4) (-0.8,-1.2) (-1.2,-1.2) (-1.3,-1.6) (-0.88,-1.7) (-0.89,-2.3) (-0.01,-1.25)
(-0.3,1.2) (-0.7,1.4) (-0.8,1.6) (-0.9,1.7) (-0.95,2.0) (0.07,0.9) (0.01,1.1) (0.03,0.8) (0.09,0.7)
(0.1,0.8) (0.2,0.4) (1.5,-0.355555) (0.9,-0.02) (-0.3,-0.01) (-0.3,-0.2) (-0.5,0.3) (-2.2,2.1)
(-2.1,1.9) (-2.4,1.8) (-2.5,0.6) (-2.8,-0.2) (-3.1,-0.5) (-3.4,0.3) (-3.6,-1.5) (-2.3,-1.7869) (-2.7,-1.7)
(-2.8, -2.3) (-3.6, -2.6);
\draw[thick,draw=red] plot [smooth,tension=1.5] coordinates{(-1.65,0.00000001) (-1.0,-0.4)
(-1.5, -0.00004) (-1.2, -0.1) (-0.9, -0.3) (-0.6, -0.3) (-0.8, -0.4) (-0.68, -0.00002) (-0.5, -0.00003)
(-0.5444, -0.3) (-0.4, -1.3) (-0.35, -1.45) (-0.4, -2) (-0.5, -1.3) (-2.1, -0.3) (-2.1, 0.1) (-2.2, -0.2)
(-1.3, -0.8) (-1.8, -1.6) (-1.9, -2.2) (-2.7, -2.6);
\draw (-5,-2.6) -- (10,-2.6){};
\draw[thick,draw=purple] plot [smooth,tension=1.5] coordinates{(-1.66,-2.2) (-1.6,-1.9) (-1.5,-2.1)
(-1.5, -1.9) (-1.3, -1.4) (-0.8, -1.2) (-1.2, -1.2) (-1.3, -1.6) (-0.88, -1.7) (-0.89, -2.3) (-0.01, -1.25)
(-0.3,1.2) (-0.7,1.4) (-0.8,1.6) (-0.9,1.7) (-0.95,2.0) (0.07,0.9) (0.01,1.1) (0.03,0.8) (0.09,0.7)
(0.1,0.8) (0.2,0.4) (1.5,-0.355555) (0.9,-0.02) (-0.3,-0.01) (-0.3,-0.2) (-0.5,0.3) (-2.2,2.1)
(-2.1,1.9) (-2.4,1.8) (-2.5,0.6) (-2.8,-0.2) (-3.1,-0.5) (-3.4,0.3) (-3.6,-1.5) (-2.3,-1.7869) (-2.7,-1.7)
(-2.8, -2.3) (-3.6, -2.6);
\node[above right=10pt of \{(-1.6,-1.2)\}] \{x_{\text{mathcal}\{I\}}\};
\end{tikzpicture}
\end{center}
\caption{\textit{$\mathrm{Sym}$ construction under $\mathscr{C} {2 {i}}}$ and
\frac{C}{2_{j + 2 \det^{\rho ime}}}. Loop configurations with distribution \frac{P}{p}, with
corresponding $+/-$ random coloring of faces in $\textbf{H}$ with distribution $\mu$, are shown
with {\color{red}red} $\gamma 1$ and {\color{purple} $\gamma 2$. Each configuration
intersects $2_j$, with crossing events occurring across the box $H_j$ and its translate $H_{j} + 2
```

\node[regular polygon, regular polygon sides=6, minimum width=6cm,label=side

\delta^{\prime}}\$. Under translation invariance, different classes of \$\mathrm{Sym}\$ domains are produced from the intersection of \$\gamma_1\$ and \$\gamma_2\$, as well as the connected component of an intersection \$x {\mathcal{|}}\$ incident to \$2 j\$. From such a configuration arrangement of \$\gamma 1\$ and \$\gamma 2\$, a magnification of the symmetric domain is provided. Across \$2_j\$, one half of \$\mathrm{Sym}\$ is rotated to obtain the other half about the crossed edge, which is enclosed by portions of \$\gamma_1\$ and \$\gamma_2\$. From paths of the connected components of each configuration, \$\mathrm{Sym}\$ is determined by forming the region from the intersection of the connected components of \$\gamma_1\$ and \$\gamma_2\$ in the magnified region. At the point of intersection between the {\color{red}red} and {\color{purple} \$+/-\$ spin configurations, the connected component associated with $x_{\mathrm{l}}\$ determines half of the lowest side of $\mathrm{l}\$. The region enjoys \$\frac{2 \pi}{3}\$ rotational invariance, and allows for the construction of identical domains under $\frac{C}_{5_j}\$ and $\frac{C}_{5_j}\$ and $\frac{C}_{5_j}\$. Connected components are only shown in the vicinity of \$2 j\$ for the identification of boundaries of \$\mathrm{Sym}\$, running from the intersection of \$\quad \quad at the cusp of \$2 \ \displays and \$3 \displays, and from two nearby intersections of \$\gamma_1\$ with \$2_j\$. Observe that \$\gamma_1\$ and \$\gamma_2\$ share a common intersection at \$x {\mathcal{I}}\$.}} \end{figure}

Without loss of generality suppose that

In the third realization of the variational formula, solutions can be fashioned towards recovering potential landscapes for the passage times through the increments of \$\tau_x\$, through the previously used formulation

 $\sum_{v \in \mathbb{Z}} \sup(Var3) = \sup_{v \in \mathbb{Z}} \sup_{v \in$

\subsection{}

Below we present further simplifications to numerical approximations of quantities associated with \$\mathcal{S}\$. Each instance is a modification of \$\textbf{(Var)}\$ (see \textit{Table 1} and \textit{Table 2}). \subsection{Isolating potential recovery terms from Var} \begin{align*} $\neq x}(v,x_1)$ $= - \int_0^{x_2} \left(\int_0^{x_2} \left($ 1 \} \mathrm{d}u \bigg) \prod_{i=2^{20} \mathrm{exp}\bigg(\frac{u^i}{i} \bigg) \mathrm{d} u \text{ } - \\ $\int_0^{x_1} \left(\int_0^{x_1} \left(\int_0^{x_1} \right) \right) dx$ $\$ \bigg) \mathrm{d} u \prod_{i=2}^{20} \mathrm{exp} \bigg(\frac{u^i}{i} \bigg) \mathrm{d} u + $\displaystyle =2}^{20} \mathrm{exp}\bigg(\frac{v^i}{i} \bigg) \mathrm{d}v \cdot (x, y)$ \end{align*} For each possible arrangement of the absorbing boundary length, through manipulation of $\label{eq:continuity} $\Delta_{\hat{S}_{v \neq x}(v,x_2) - \mathcal{S}_{v \neq x$ x\(v,x_1)\\$, terms from the unknown potential can be recovered with the following rearrangements.

\subsubsection{

}

Substitution yields,

\begin{align*}

\subsubsection{}

Substitution yields,

\begin{align*}

\subsection{ $x_2 > x_1, x_1 > 1$ }

\noindent while for $v \neq x_1$ and $v > x_1$, the second term corresponding to each possibility in $\Delta \{x_1 = x_1 \}$ is of the form,

\begin{align*}

 $\label{limit_0^{x_2} \left(u^i}_{i=2}^{20} \operatorname{exp}\bigg(\frac{u^i}{i} \bigg) \right) $$ \operatorname{d} u \ \operatorname{exp}\bigg(\frac{v^i}{i} \bigg) \operatorname{d} v \ \operatorname{ext} , \ \ \operatorname{align^*} $$$

\noindent and

\begin{align*}

\noindent respectively. We collect like terms which are taken over the same region of integration. This requires that we identify rearrangements of terms in each subcase below.

\subsubsection{\$v \equiv x_1\$}

\noindent Under this assumption, the relation takes the form,

\begin{align*}

\noindent resulting from an application of \$\textbf{(Lin2})\$ to the third term which yields

```
\begin{align*}
```

```
\begin{align*}
```

 $- \int_0^{x_2} \left(\frac{i=2}^{20} \operatorname{exp} \left(\frac{u^i_2}{i} \right) - 1 \right) \\ - \int_0^{x_2} \left(\frac{i=2}^{20} \operatorname{exp} \left(\frac{u^i_2}{i} \right) - 1 \right) \\ - \int_0^{x_2} \left(\frac{i=2}^{20} \operatorname{exp} \left(\frac{u^i_2}{i} \right) - 1 \right) \\ - \int_0^{x_2} \left(\frac{i=2}^{20} \operatorname{exp} \left(\frac{u^i_2}{i} \right) - 1 \right) \\ - \int_0^{x_2} \left(\frac{i=2}^{20} \operatorname{exp} \left(\frac{u^i_2}{i} \right) - 1 \right) \\ - \int_0^{x_2} \left(\frac{u^i_2}{i} \right) \\ - \int_0^{x_2} \left(\frac{u^i_2}{i}$

\noindent while for the first term applying the rearrangement to the innermost variable yields,

\begin{align*}

\begin{frame}{overview of the Brewster et al paper}

this paper from the Phillips lab at Caltech (in {\color{gray}gray} from a previous slide), proposes studying various transcription factors in the genome by

\begin{itemize}

\item[\$\bullet\$] quantifying thermodynamic determinants to the binding process, by counting admissible configurations of binding through a multiplicative factor to the protein fold change which is proportional to the number of repressors in the cell with the size of the nonspecific binding reservoir,

\item[\$\bullet\$]

\item[\$\bullet\$] finally, apply the analysis routines within the Cas family, to measure the native conformations to proteins within the family \end{itemize}

\end{frame}

\end{frame}	
\begin{frame}{building profiles of the stopping time of the random walk}	

https://cornell.zoom.us/j/4896239706?pwd=UU15R3l3S05ucnpwa3hpUHI5ZzJwUT09

It's great to hear from you. Sorry if the message is quite long but I wanted to tell you about the past few weeks. I had to cut a bit out of the PDF so that it captures some precise computations that we can do, which we can simulate for predictions for new data (whenever it comes before or after December because I wanted to submit for the March meeting and stick around anyways).

I'm sure that you have been extremely busy, and I have future plans for independent work on the draft as everybody's schedule is becoming even more hectic with the students leaving soon, and professors having to arrange for wrapping up the semester.

Some time ago, I thought about ways that I could further work on the draft. After some thought, I was very sure that you would want us to include discussions of the ODE that we briefly mentioned in the lab meeting together from my slides and your notes, so I have devoted another

page to introduce the equation and its solutions for the specific class of potentials that I mentioned in the presentation. [I strongly think that this can be helpful for the direction that you wanted to take the project in.]

I also found a much, much more clear way of rewriting the solution than what I had in the previous set of slides (the expression is similar, but the thing that confused me was what I call the "intermediate" variables for the potentials u 1 & u 2).

Beyond the second page, I also introduced the variational formulae (at least that's what I call them because we can observe perturbations in exit times) which would allow us to solve the inverse problem that I have defined. [The approach can allow for us to look at several different possibilities from the "ansatz distribution," a term that I have devised to denote the distribution of possible exit times that we can choose to measure the perturbation of the potential in the binding landscape.]

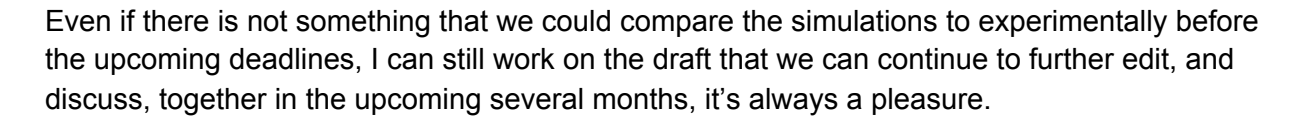
Best,			
Pete			

Again, apologies if the last message was long but I wanted to provide you with a good amount of detail so that you could very briefly look over the draft in light of the motivation that we described in the last lab presentation.

I was wondering if you think that there is additional experimental data from David's work for Cas9 (or any other data) that we can analyze from this perspective? I have other very brief questions for 5 minutes or so, if the coffee hour is up for Friday morning or if another time to meet, very briefly, works for you. Sorry, it's hard for me to always get up that early on NY time lol, but I could try for Friday if the hour is still going on.

In particular, how would you recommend that I construct the partition function from the \Nabla gradient probability measure? We could use the Z from David & Sue's paper but maybe you wanted me to reformulate that part of the measure too. I have significantly built upon the exit time formalism that you recommended I study.

I just wanted to raise these questions because I am also working on other work that I am shooting to submit for the Mathematics PhD application. I'll end up sending you all my "sample" drafts anyways as they are in preparation, but the time is running short as I continue working (I'll have 3 other drafts rather than this one) and I'm trying to prioritize my time efficiently. I have also been studying the dilute Potts model (loop O(n) model, high temperature expansion of the spin O(n) model) with conjectures from Nienhuis and have been making progress in the Proofs & arguments, and I want to display my knowledge of different areas of statistical mechanics to the committees.



All the best,

Pete

Besides the rectangular crossings, to create symmetric domains for the proof additional crossing events measurable under \$\mu\$ are of the form,

To study numerically well posed measures on readouts from quantum circuits,

 $\label{thm:linear:construction} $$\operatorname{B}^{j}_{\mathrm{B}_1}, \mathscr_{B}^{j}_{\mathrm{B}_2}, \mathscr_{B}^{j}_{\mathrm{B}_3}, \mathscr_{B}^{j}_{\mathrm{B}_2}, \mathscr_{B}^{j}_{\mathrm{B}_3}, \mathscr_{B}^{j}, \mathscr_{B}^{j}_{\mathrm{B}_2}, \m$

```
\begin{align*}
\mathcal{C^{\prime}}_{1 \rightarrow 2} = \{ 1 \overset{H}{\longleftrightarrow} 2 \} \\
\text{ } \backslash \text{ } \mathcal{C}_{1 \rightarrow 2} \text{ } \text{ } \\
\mathcal{C}^{\prime}_{1 \rightarrow 3} = \{ 1 \overset{H}{\longleftrightarrow} 3 \} \\
\backslash \text{ } \mathcal{C}_{1 \rightarrow 3}, \mathcal{C}^{\prime}_{1 \rightarrow 5} = \\ 1 \overset{H}{\longleftrightarrow} 5 \} \\
\text{ } \backslash \\
\text{ } \mathcal{C}_{1 \rightarrow 6} = \\ 1 \overset{H}{\longleftrightarrow} 6 \\
\text{ } \mathcal{C}^{\prime}_{1 \rightarrow 6} \\
\text{ } \mathcal{C}_{1 \rightarrow 6} \\
\text{ } \m
```

```
\begin{figure}[tb]
                                                       \centering
                       \includegraphics[width=1\columnwidth]{FS.eps}\\
 \caption{To more closely analyze the behavior of the series approximation from which
 predictions will be generated with a corresponding MSE, the behavior of the series
 approximation, as $t$ varies, is depicted above. }
 \end{figure}
\begin{tabular}{|p{4.5cm}||p{4.5cm}|p{4.5cm}|p{4.5cm}|
    \hline
    formula& $\tau_1, \tau_2$& approximation term&recovered potential \\
    \hline
                   & & $\int $ & \\
                   \hline\hline
 \end{tabular}
 Furthermore, to address different qualities of the readout problem, we introduce \textit{shallow}
 observables}, which are defined to be quantities which
 \noindent while for $v \equiv x$,
\begin{align*}
                   \label{eq:conditional} $$\operatorname{S}_{v = x}(v,x)  \cdot 0^{x}  \cdot i_{0}^{x} \cdot i_{0}^{x}
 \bigg)\bigg(\int_0^x \end{i=2}^{20} \mathbf{0} \operatorname{leg}(\frac{u^i}{i} \cdot \frac{u^i}{i} \cdot \frac{u^
 \bigg) \mathrm{d} u \text{ . } \\
 \end{align*}
 \subsubsection{$v \equiv x_2$}
```

\noindent Under this assumption, the relation takes the form,

```
\begin{align*}
                \boxed{ \int_0^{x_1} \int_0^{x_1} }
                                                                                                                                         \displaystyle \frac{i=2}^{20} { \mathrm{sp}\left( - \frac{u^i}{i} \right)}
\bigg) - \mathbf{\{i=2\}^\{20\}}
\ensuremath{2 \prod_{i=2}^{20} \mathrm{20} \operatorname{exp}\bigg(\frac{u^i}{i} \bigg) - 1 \ \mathrm{d}u \bigg) \ \cdots }\
\prod_{i=2}^{20} \mathrm{exp}\bigg( \frac{u^i}{i} \bigg)
                  \mathrm{d} u } \tag{\textbf{Var3B}} \text{ , } \\
\end{align*}
\subsubsection{$v \equiv x_1$}
Rearrangements yield,
\begin{align*}
              \mathrm{exp}\bigg( \frac{u^i}{i}\bigg) -1 \}
                                                                                                                                                     \mathrm{d} u \text{ } \prod_{i=2}^{20}
\mathrm{exp}\bigg(\frac{v^i}{i} \bigg) \text{ } \mathrm{d}v \text{ } + \cdots } \\
              \boxed{ \in 0^{x_2} \Big| ( \int_{x_2}^{x_1} {\rho _{i=2}^{20}} \Big| 
\mathrm{exp}\bigg(\frac{u^i}{i} \bigg) - 1 \ \mathrm{d} \ u \bigg) \ \prod_{i=2}^{20}
\mathrm{exp}\bigg(\frac{v^i}{i} \bigg) \mathrm{d} v \text{ } } \text{ . } \tag{\textbf{Var1B}}\\
\end{align*}
\subsubsection{$ v \equiv x_1$}
Under this assumption we invoke \textbf{(Lin2)}, from which the variational formula takes the
form,
\begin{align*}
        - \int_0^{x_2} \operatorname{d_{i=2}^{20} \operatorname{exp} \operatorname{d_{i}_{i}} \operatorname{d_{i}_
\[ =2 ^{20} \mathbb{C} \right) \
```

\noindent from which an application of \$\textbf{(Lin2)}\$ to the second term yields,

\begin{align*}

\noindent implying that

\begin{align*}

 $\sum {v > x_1}$

Under this assumption, we invoke \$\textbf{(Lin2)}\$ in the second term, after which invoking \$\textbf{(Lin1)}\$ in the second term, and subsequent rearrangements with the third term yields

\begin{align*}

```
\label{thm:condition} $$ \operatorname{textbf}(Lin1)}_{Rightarrow} \in _0^{x_2} \bigg( \int_0^{x_1} \operatorname{i=2}^{20} \operatorname{textbf}(Lin1)}_{Rightarrow} \right) \\ \operatorname{text}_{x_1}^{x_2} \operatorname{i=2}^{20} \operatorname{textbf}(Lin2)}_{ii} \bigg) \\ \operatorname{text}_{x_1}^{x_2} \operatorname{textbf}(Lin2)}_{ii} \bigg) \\ \operatorname{text}_{x_1}^{x_2} \bigg) \\ \operatorname{text}_{x_2}^{x_2} \bigg) \\ \operatorname{text}_{x_1}^{x_2} \bigg) \\ \operatorname{text}_{x_2}^{x_2} \bigg) \\ \operatorname{text}_{x_2
```

 $\label{liminu} $$ \inf_{x_1}^{x_2} \left(i=2\right^{20} \operatorname{exp}\bigg) \left(-\frac{u^i}{i} \right) \mathrm{d} u \ \ \left(i=2\right^{20} \operatorname{exp}\bigg) \mathrm{exp}\bigg) \mathrm{d} v \text{ . } \ \end{align*} $$$

\noindent We obtain intermediate terms of the relation,

\begin{align*}

 $- \int_0^{x_2} \left(x_2 \right) \left(x_2 \right) \left(x_2 \right) \left(x_2 \right) \left(x_1 \right) \left$

\noindent for integral terms that are uniform in the boundaries of integration on each order, while the remaining terms are of the form,

\begin{align*}

\noindent are composed of nonuniform bounds on each order order of integration. Applying Fubini to either integral above permits for consolidation of the mixed ordered terms. Putting together all rearrangements implies,

\begin{align*}

```
\label{thm:cond} $$ \operatorname{-\int_0^{x_2} \left( \operatorname{i=2}^{20} \operatorname{i=2}^{20} \operatorname{i=2}^{20} \operatorname{i=2}^{20} \operatorname{i=2}^{20} \operatorname{i=2}^{20} \operatorname{i=2}^{20} \operatorname{int}_0^{x_1} \operatorname{int}_0^{x_1} \operatorname{i=2}^{20} \operatorname{i=2}^{20} \operatorname{int}_0^{x_1} \operatorname{int}_0^{
```

```
Rearrangements yield,
```

```
\begin{align*}
                                \boxed{\int_0^{x_2} \inf_0^{x_2} \left( \frac{i=2}^{20} \mathcal{E}_0^{1} \right) } \boxed{\int_0^{x_2} \left( \frac{i=2}{2} \mathcal{E}_0^{1} \right) } \boxed{\int_0
- \mathrm{exp}\bigg( \frac{u^i_2}{i} \bigg) + 1 \} \mathrm{d} u_2 \prod_{i=2}^{20}
\mathrm{exp}\bigg(\frac{u^i 2}{i} \bigg) \mathrm{d} u 2 \text{} + \cdots } \\
                                 \label{limit_0^{x_1} \inf_0^{x_1} {\rho^{i=2}^{20} \operatorname{lex}(\frac{1}{i})} int_0^{x_1} {\rho^{i=2}^{20} \operatorname{lex}(\frac{1}{i})} int_0^{x_1} int_0^{
u_1 + \int_0^{x_1} \int_0^{x_2} \sqrt{20} \operatorname{exp}\big(-\frac{1}{i} \big) \
\mdthrm{d} u_1 \ \prod_{i=2}^{20} \mdthrm{exp}\bigg(\frac{u^i_1}{i} \bigg) \mdthrm{d}u_1 \ \text{}
. } \tag{\textbf{Var1A}}\\
\end{align*}
\subsubsection{$v \equiv x 2$}
Under this assumption the variational formula takes the form,
\begin{align*}
        \boxed{ \in 0^{x_2} \inf_0^{x_2} \left( i=2\right^{20} \mathbb{e}^{20} \right) - \cong (i=2)^{20} \cong (i=2)^{20}
\mathrm{exp}  \frac{u^i}{i}  bigg) + 1 \} \mathrm{d}u \prod_{i=2}^{20}
\mathrm{exp}\bigg(\frac{v^i}{i} \bigg) \mathrm{d} v + \int_0^{x_1} \operatorname{d} v + \int_0^{x_1} \mathrm{d} v + 
\label{limit} $$\operatorname{exp}\bigg(\frac{u^i}{i} \bigg) \bigg(\int_0^{x_1} {2 \left(\frac{i-2}^{20}\right)} \
\mathrm{exp}\bigg(\frac{u^i}{i} \bigg) - 1 \} \mathrm{d}u \bigg) \mathrm{d} u }
\tag{\textbf{Var2A}} \text{ . }\\
\end{align*}
\renewcommand{\arraystretch\{6}
\renewcommand{\tabcolsep}{8mm}
\begin{table}
                  \begin{tabular}{|c|c|c|c}
                                     \hline
                                     \large Formula & \large $\tau_1, \tau_2$ & \large Numerical evaluation& \large Potential \\
                                     \hline
                                        Var$2$C & & \multicolumn{1}{m{3cm}|} \huge $\int $ }
                                                                                                                                                                                                                                                                                                                                                                                                                                                                                                 \\ &
                                     \hline
```

```
\hline
\Var $3$A & & \multicolumn{1}{m{3cm}|}{ \huge $\int $ } & \\
\hline
\hline
\Var $3$B & & \multicolumn{1}{m{3cm}|}{ \huge $\int $ } & \\
\hline
\hline
\hline
\hline
\hline
\hline
\hline
\end{tabular}
\end{tabular}
```

To more easily describe connectivity between

a trapezoidal partition of $\mathrm{H}\$ into upper and lower halves will be introduced through the decomposition $\mathrm{H}\$ mathscr $\{T\}_{-} \subset T_{-}$

There were some aspects of the argument that I deliberately held back on in our past discussion, because I needed to read about the argument from some of the pages that we discussed. I have been working to fill in more of those details, and they definitely provide characteristics of the loop model that have not been previously mentioned.

Standard computations of exit times surround numerical routines to determine characteristics of the energy landscape in which CRISPR proteins participate, including stages of the binding process comprised of protein inspection of target sequences for complementarity, in which successful binding occurs through the formation of a stably bound complex. In this work, an IVP associated with a stochastically driven oscillator for the exit time will be presented, from which exit times for varying potential landscapes are obtained. To build upon previous formulations of potential landscape recovery from distributions of exit times in the landscape, we also will discuss novel numerical schemes from which fluctuations to the binding landscape can be realized. The scheme primarily relies on establishing relations between numerical approximations of exit times, in turn enabling us to reconstruct a potential landscape which is valuable for constructing probability measures to quantify likely configurations of different proteins within the Cas family throughout the binding process. Time permitting, comparisons will be established between other statistical mechanics approaches.

I have added in some more details in <u>Section 4.2</u> because the crossing events themselves need to be indexed by some variable j, as the authors do in the planar case for the random cluster model. The modification that I had to introduce makes the crossing events more complicated, but at the same time allows for us to generalize these steps of the argument by looking at "hexagonal triplets" which are similar to the crossing events defined in the simpler planar case (I added in some pictures because they easily show how the connected components of the paths for these events should appear).

Although it appears that there may be a lot of text in <u>Section 4.2</u>, and I can have a reputation for writing a bit, I feel that it is necessary to clearly define what I am doing before proving the separate cases of the union bound. It makes it extremely clear how the argument differs, and illustrates some brief remarks that I made earlier. I feel that it is organized more clearly than how it appears in the original paper, they seem to write some things quickly over there. [There are also two small typos on Page 15 of their paper, and I reflected more clearly on this confusion with the notation in the most updated draft. That part of the paper confused me for some time; the arguments in my draft take into account 2 pi / 3 rotational invariance of the loop measure.]

I also thought more about the cases in the Proof for the argument for constructing the symmetric domains. As I expected, we have to consider more cases for the generalization, which I have

studied. The additional cases are complicated because of the regions that are "left over" in the hexagonal translates [the illustration for "hexagonal triplets" on the top of Page 6 highlights how we would horizontally translate the hexagons to obtain similar crossing events that HDC & VT used, but there are still complications that I have discussed on the bottom of Page 5 which carry on for several pages after.]

Here are some nontrivial details that we could briefly discuss:

- The symmetric region is actually larger than the region over which the crossing probabilities are quantified.
- Applying the argument in the second case given by HDC & VT across the hexagons that
 I have illustrated in the picture entails that we form symmetric domains about particular
 edges of the hexagon. This part of the argument is actually quite interesting, because we
 have to pushforward the intersection of <u>closely define crossings</u> that are given on Pages
 7 and forwards.
- Wrapping up the Proofs with a few more arguments, which HEAVILY rely on the comparison between boundary conditions on the loop measure.

Maybe it's a good thing if you didn't look at the previous draft yet because once I have more I think the direction will become more clear. I'm trying to build up separate results in my physics papers for some other "tricks" up my sleeve,

Pete			

Again, sorry if my past message was long. I know that these times must be busy & difficult for everybody.

I wanted to give you an idea of what we would have to include in the argument for the generalization. The steps have become more clear, and I wondered why parts of it had not clicked in sooner. The difference emerges primarily in the comparison between boundary conditions that I mentioned last time, but also on the spatial/domain markov property which has been under different circumstances has been used to study Glauber dynamics of the Ising model from other probabilists in the field.

I was wondering if you have a little time again this upcoming weekend to very briefly discuss future steps, and to tell you about qualities of the symmetric domains for the loop model. A good heuristic for difference in the argument is that there is "more than one way for loop configurations to turn right or left" (this will be completely clear later, I promise).

There are not many pages in the original Renormalization paper left to generalize for dilute Potts and I think that I can meet my goal. Further details and more subtle points about the novelty of the Proof should become much more clear. To "open" up the argument more than they did for the random cluster model, I included illustrations of a few types of symmetric domains, it's quite an interesting argument, and helps us understand how assumptions on the measure of configurations from the ensemble influence the probability of obtaining very similar crossing events.

I can cut down the time of the meeting to 15 minutes if last time at 25 mins was too long for you. [I have also included diagrams to show how the WEAKER form of the Domain Markov property applies to the loop model.]

```
My best,
Pete
\begin{center}
\begin{tikzpicture}
 \newdimen\R
\R=2.2cm
 \draw (0:\R)
 foreach \ x in \{60,120,...,360\} \{ -- (\x:\R) \}
-- cycle (360:\R) node[right]
-- cycle (300:\R) node[below]
   -- cycle (240:\R) node[below] ${(v_1)}$
-- cycle (180:\R) node[left] ${(v_2)}$
-- cycle (120:\R) node[above]
       -- cycle (60:\R) node[above];
       \newdimen\R
\R=2.6cm
 \draw (0:\R)
 foreach \ x in \{60,120,...,360\} \{ -- (\x:\R) \}
-- cycle (360:\R) node[right]
-- cycle (300:\R) node[below]
    -- cycle (240:\R) node[below]
-- cycle (180:\R) node[left]
-- cycle (120:\R) node[above]
       -- cycle (60:\R) node[above];
\end{tikzpicture}
```

\end{center}			

Besides demonstrating that this step of the novel renormalization argument heavily depends on the probability of a horizontal crossing in the regimes \$\rho \equiv 1\$ \$\& \text{} \rho >2\$, difficulties associated with the hexagonal analogue of a long horizontal crossing

I have attached the finalized slides for the next presentation. I thought that it is best if I give the presentation first in the lab meeting, to then directly hear from you with your thoughts before writing the introduction & moving forwards. So I held off from editing the document that I sent over from last week. I also ended up including some slides on the other approach, from insights on your suggestion to study mean exit times. I have identified areas which, to the best of my knowledge, have not been studied yet by other researchers in the literature. I still believe that I can make use of previous slides but for now they are not included.

Even if I spend around a minute or so per slide, I have quite a bit of material to discuss that draw upon your new suggestion, in addition to previous discussions. I'll discuss how my approach is novel and how we can build up more results from this starting point. It's a presentation that I'm definitely proud of (my longest one), and was a good direction to pursue from your advice. I had to record for another set of slides for a different presentation earlier.

Let's talk more over Zo	oom in the la	ib meeting after	I present,
-------------------------	---------------	------------------	------------

Pete			

Hope that you have been well. Thanks for the discussion yesterday in the lab meeting.

In particular, maybe one thing that I forgot to briefly mention in the spur of the moment was if there is a preference that you have for the method that we use to compute the passage times. In the slides I discussed 2 approaches, one which is very closely related to the one found in the Utah notes, while the other method is raised in the spirit of the inverse problem of reconstructing potentials from visit time distributions from a 2004 paper. The expressions for \tau_2 - \tau_1 that I got from rearranging terms from the solution. I have attached an update to the draft with a page describing the grounds for generalization from your previous paper.

I was just wondering what you think is best, and wanted to hear your thoughts before working more.

Take care,
Pete
\begin{frame}{constructing potentials to obtain mean exit times for other potentials}
\end{frame}
\begin{frame}{identifying candidate potentials}
throughout the protein inspection phase, comparison of base pairs, regardless of agreement, the first passage times,
\begin{itemize} \item[\$\bullet\$] should be collected for different potentials and then averaged over the number of trials to determine the mean first passage time,
\item[\$\bullet\$] in the case of {\color{blue}Cas12a}, should be computed against a potential that reflects more substantial energetic barriers for the first \$6\$ base pairs of the sequence, while the remaining base pairs in the sequence will reflect aspects of protein folding potentials in references (to be introduced),
\item[\$\bullet\$] should differ on meaningful orders of magnitude in time, namely on the order of magnitude of a fraction of a second,
\item[\$\bullet\$] can be implemented for different proteins within the Cas family through the implementation of solving for the mean exit times, with a potential choice which assigns different energetic barriers to different base pairs along the \$20\$ bp sequence \end{itemize}

\end{frame}

\begin{frame}{difficulties associated with the energy landscape}

\begin{itemize}

\item[\$\bullet\$] potentially large order parameter search to the native state,

\item[\$\bullet\$] means of potential construction that is physically inclusive of all stages of protein binding, with particular attention towards the protein folding stage, which can be analyzed for different proteins by identifying the base pairs of the sequence that are responsible for initiating the folding stage,

\item[\$\bullet\$] characteristics of the native state that are universal across a family of proteins, if any \end{itemize}

\end{frame}

\begin{frame}{criterion for generating appropriate simulation trajectories}

to test different subsets of the binding energy landscape, similar approaches to determine the first mean exit times can be modified to study the distribution of passage times up to a base pair of interest, which across Cas proteins would vary across base pairs of the target sequence, as a result requiring that:

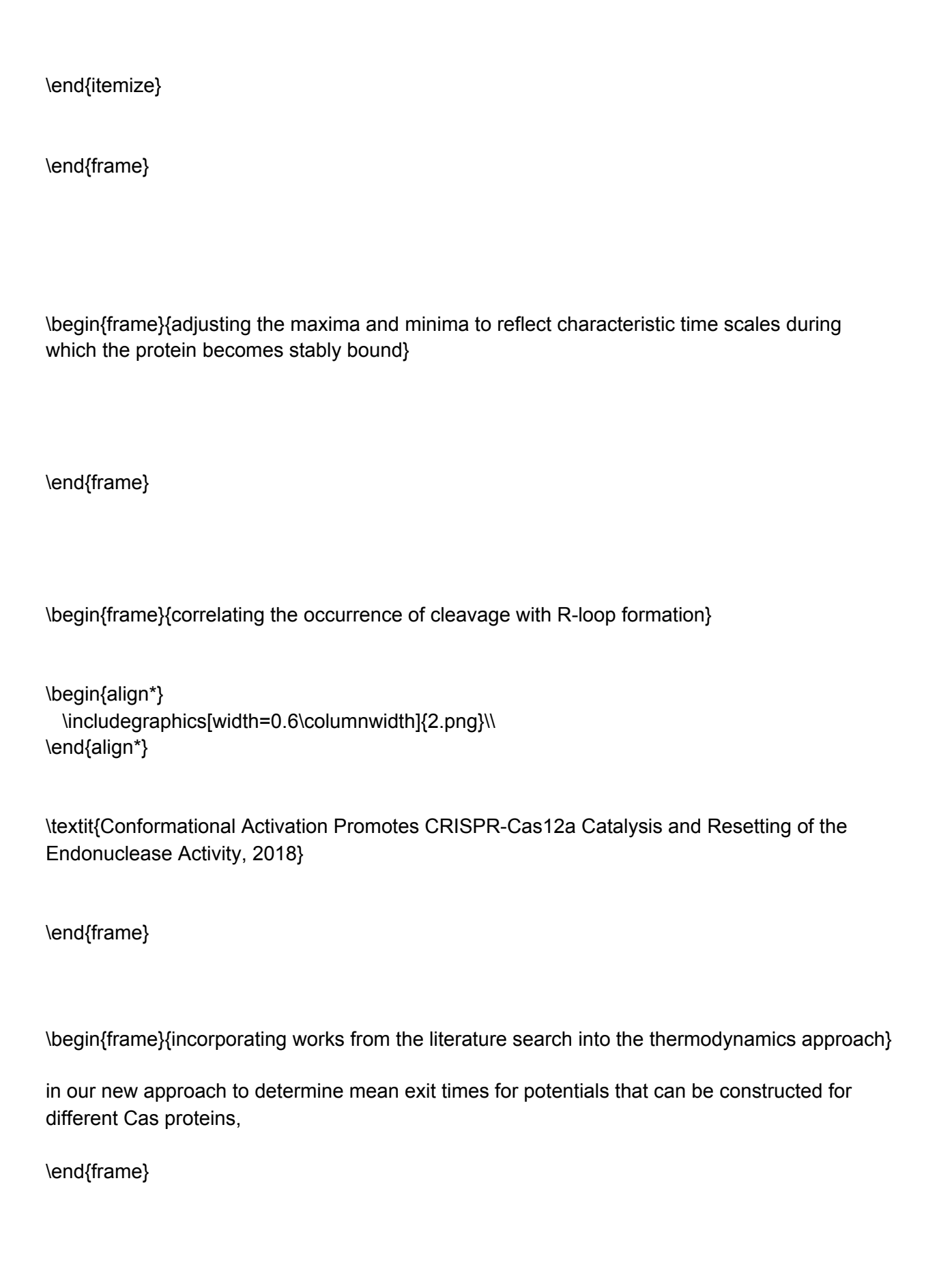
\begin{itemize}

\item[\$\bullet\$]

\item[\$\bullet\$] parameter schemes be developed through adjustment of the magnitude of the exponentials in the partition function,

\item[\$\bullet\$]

\item[\$\bullet\$] comparisons between different proteins within the Cas family can be established by



\begin{frame}{thermodynamic insight}
\end{frame}
\begin{frame}{plans for the upcoming weeks}
\end{frame}
\int_0^{t_{\mathrm{crit}}} \int_0^{t_{\mathrm{crit}}} - + 1\text{,}
\begin{frame}{one method: potential preparation}
on the basis of different binding sequences, mean first exit times will be computed for
\begin{itemize} \item[\$\bullet\$] diffusion processes involved in the Brownian motion of particles as the DNA bubble is formed for binding, by
\begin{itemize}
\item[\$\bullet\$] constructing the oscillator of interest for each sequence,

\item[\$\bullet\$] enforcing a suitable choice of the potential energy landscape in front of the first derivative term which is reflective of base pair matches and mismatches between the guide and target sequences,

 $\label{thm:condition} $$ \operatorname{solutions} of the aforementioned form, from which mean exit times can be approximated$

\end{itemize}

\end{itemize}
\end{frame}
\begin{frame}{towards more complexity in the potential}
counterintuitively, enforcing potentials with more than one term simplifies integral terms (from previous slides), in the sense that:
\begin{itemize} \item[\$\bullet\$] \$2\$ of the terms that appear as Gamma functions \textbf{in potentials of the simpler type} are instead exponentials whose powers consist of polynomials, allowing for numerical approximations
\item[\$\bullet\$] albeit potentially more costly, comparison of the change in solutions to the differential equation demonstrates aspects of our strategy for construction potentials in the first place
\end{itemize}
\end{frame}
\begin{frame}
in turn, it is necessary to
\begin{itemize} \item[\$\bullet\$] recognize the tradeoff between the first mean exit time and candidate potentials of the energy landscape, which in the case of previous computations, demonstrates that

\begin{itemize}

\item[\$\bullet\$] numerically, while the power of one of the exponentials in each of the \$2\$ terms in the solution to the differential equation differ, the exclusion or inclusion of Gamma function terms reflects a difference in mean exit times,

\item[\$\bullet\$] in addition to a difference in the mean exit time between different choices of a potential

•
\end{itemize} \end{itemize}
\end{frame}
\begin{frame}{incorporating thermodynamic qualities into the potential}
in line with previous thermodynamics interpretations, base pair mismatches
\begin{itemize} \item[\$\bullet\$] impacts the threshold binding energy so that the protein can successfully bind which is characteristic of \textbf{sharp} phase transitions,
\item[\$\bullet\$] can be tuned so that the transition probabilities resulting from a \textbf{single} base pair mismatch
\item[\$\bullet\$]
\end{itemize}
\end{frame}
\begin{frame}{path dependence}
\end{frame}
\begin{frame}{prescription}

heuristically from our illustration modifying the portion of the genome for which the energy landscape achieves a local maxima

٠			•••		•
١	haa	ıın.	lita.	mız	Δl
1	beg	111 15	שווכ	пп∠	ᇊ

\end{frame}

\item[\$\bullet\$] impacts the minimum binding energy for all base pairs after the mismatch has occurred,

\item[\$\bullet\$]
\item[\$\bullet\$]
\item[\$\bullet\$]
\end{itemize}
\end{frame}
\begin{frame}{related works in the literature}